

doi: 10.12029/gc20160607

刘建峰, 李锦轶, 孙立新, 等. 内蒙古巴林左旗九井子蛇绿岩锆石U-Pb定年: 对西拉木伦河缝合带形成演化的约束[J]. 中国地质, 2016, 43(6): 1947–1962.

Liu Jianfeng, Li Jinyi, Sun Lixin, et al. Zircon U-Pb dating of the Jiujingzi ophiolite in Bairin Left Banner, Inner Mongolia: Constraints on the formation and evolution of the Xar Moron River suture zone[J]. Geology in China, 2016, 43(6): 1947–1962(in Chinese with English abstract).

内蒙古巴林左旗九井子蛇绿岩锆石U-Pb定年: 对西拉木伦河缝合带形成演化的约束

刘建峰^{1,2} 李锦轶¹ 孙立新³ 殷东方¹ 郑培玺^{2,4}

(1. 中国地质科学院地质研究所, 北京 100037; 2. 东北亚矿产资源评价国土资源部重点实验室, 吉林 长春 130061;
3. 中国地质调查局天津地质调查中心, 天津 300170; 4. 吉林大学地球科学学院, 吉林 长春 130061)

提要:本文对位于西拉木伦河蛇绿岩带东段的九井子蛇绿岩中辉长岩脉以及蛇绿岩的围岩开展了锆石U-Pb定年。结果表明辉长岩的形成时代为(274.7 ± 1.7) Ma, MSWD=0.079, 属于早二叠世晚期;结合前人地层、古生物、岩浆岩等方面的数据, 表明内蒙古东南部早二叠世晚期还可能存在大洋盆地。与九井子蛇绿岩呈断层接触的粉砂岩碎屑锆石年龄大致构成4个峰值:2350~2700 Ma、1700~2100 Ma、370~470 Ma和250~290 Ma, 通过与区域构造热事件的对比分析, 表明其物源主要来自中朝古板块的北缘。粉砂岩中最小的锆石年龄为晚二叠世末—早三叠世初((249 ± 4.7) Ma), 该年龄与内蒙古东南部海相地层消失的时代、安加拉植物群和华夏植物群出现混生的时代、西伯利亚和中朝古板块古纬度曲线收敛的时代以及区域上与碰撞相关的岩浆岩形成时代大致相同, 据此本文认为九井子蛇绿岩的构造侵位时代应为晚二叠世末—早三叠世初, 同时也可能代表古亚洲洋的最终闭合时代。

关 键 词:内蒙古东南部; 西拉木伦河蛇绿岩; 构造演化; 古亚洲洋; 锆石U-Pb定年

中图分类号:P597³; P588.12⁴ 文献标志码:A 文章编号:1000-3657(2016)06-1947-16

Zircon U-Pb dating of the Jiujingzi ophiolite in Bairin Left Banner, Inner Mongolia: Constraints on the formation and evolution of the Xar Moron River suture zone

LIU Jian-feng^{1,2}, LI Jin-yi¹, SUN Li-xin³, YIN Dong-fang¹, ZHENG Pei-xi^{2,4}

(1. Institute of Geology, Chinese Academy of Geological Sciences, Beijing 100037, China;
2. Key laboratory of Mineral Resources Evaluation in Northeast Asia, Ministry of Land and Resources, Changchun 130061, Jilin, China; 3. Tianjin Center of Geological Survey, China Geological Survey, Tianjin 300170, China; 4. College of Earth Science, Jilin University, Changchun 130061, Jilin, China)

Abstract: The Jiujingzi ophiolite belongs to the eastern segment of the Xar Monron River ophiolite belt in southeastern Inner Mongolia. In this paper, the authors carried out zircon U-Pb dating of a gabbro dike of the Jiujingzi ophiolite and the surrounding

收稿日期:2016-08-04; 改回日期:2016-08-25

基金项目:国家自然科学基金项目(41102029, 41472055)和中国地质调查局地质调查项目(12120115069301, DD20160201-01)联合资助。

作者简介:刘建峰,男,1981年生,副研究员,从事岩石学和岩石地球化学研究;E-mail: wenjv@aliyun.com。

siltstone that is in fault contact with the ophiolite. The results indicate that the gabbro dike was formed in late Early Permian (274.7 ± 1.7 Ma, MSWD=0.079). Considering previous geological data on strata, paleontology and magmatic rocks, the authors hold that there was still an ocean basin in late Early Permian in southeastern Inner Mongolia. The detrital zircons of the adjacent siltstone constitute four age peaks: 2350–2700 Ma, 1700–2100 Ma, 370–470 Ma and 250–290 Ma. A comparison with regional tectono-thermal events shows that the provenance of the siltstone was mainly from the north margin of the Sino-Korean paleoplate. The age of the youngest zircon is late Early Permian–early Early Triassic (249 ± 4.7 Ma), which is similar to the ages of the disappearance of the marine strata in southeastern Inner Mongolia, the mixing between the Cathaysian and Angaran floras, the convergence of the palaeolatitude curves of the Siberian and Sino-Korean paleoplates and the formation of the collision-related magmatic rocks. It is thus suggested that the tectonic emplacement of the Jiujingzi ophiolite might have occurred in late Early Permian–early Early Triassic, which might represent the final closure time of the Paleo-Asian Ocean.

Key words: southeastern Inner Mongolia; Xar Moron River ophiolite; tectonic evolution; Paleo-Asian Ocean; zircon U-Pb dating

About the first author: LIU Jian-feng, male, born in 1981, associate researcher, majors in geochemistry, engages in research on igneous petrology and geochemistry; E-mail: wenjv@aliyun.com.

Fund support: Supported by National Natural Science Foundation (No. 41102029 and 41472055), Geological Survey Project of China Geological Survey (No. 12120115069301, No. DD20160201-01).

北亚造山区南部,又称“阿尔泰造山带”或“中亚造山带”,是指位于西伯利亚古陆与塔里木和中朝两个古陆之间的宽广地区^[1]。已有研究表明,该造山区是全球新元古代—显生宙以来地壳增生和改造最为显著的地区,也是世界上矿产资源潜力最大的地区,因而北亚造山区南部地壳的构造分区和演化一直是国内外学者关注和研究的焦点^[1-11]。内蒙古东南部地区位于北亚造山区的东南部,以发育该造山区南部最年轻的海相沉积岩系以及贺根山、索伦山、西拉木伦河等多条蛇绿岩带为特征,被认为是西伯利亚和中朝古板块之间的古亚洲洋最终闭合的地区^[1-3, 8-9, 12-20]。目前,索伦山蛇绿岩带作为两大古板块缝合带的认识已得到广大研究者的认同,然而两大古板块最终碰撞拼合的时代以及索伦山蛇绿岩带向东如何延伸仍存在较大的争议。

一些学者依据内蒙古东南部石炭一二叠纪古生物群的地理分区、杏树洼蛇绿岩带硅质岩中的二叠纪放射虫化石、二叠纪火山岩的时空分布和岩石组合、古地磁学以及构造变形等方面的数据,认为西拉木伦河蛇绿岩带代表西伯利亚和中朝古板块的最终缝合带^[12, 17, 21-25]。另一些学者虽然也赞同两大古板块在中一晚二叠世闭合,但认为缝合带应位于林西县北部的盖家店—八楞山一带^[8-9, 15-16]。还有一些学者认为贺根山蛇绿岩带是两大古板块的最终缝合带,并依据苏尼特左旗地区上泥盆统与下伏地质体的不整合关系、与蛇绿岩伴生的泥盆纪地层

中发现的珊瑚和放射虫化石以及全岩 Sm-Nd 等时线年龄(403 Ma)认为板块碰撞拼合时代为泥盆纪或早石炭世^[2-3, 13-14, 26-29]。此外,还有一些学者提出缝合带位于贺根山和西拉木伦河蛇绿岩带之间的艾力格庙—锡林浩特一带,闭合时代为中泥盆世之前,而北亚造山区南部二叠纪海相盆地形成于裂谷环境^[30-32]。

作为大洋岩石圈的残余,蛇绿岩是划分古板块边界的重要依据。以往的研究中多依据与蛇绿岩伴生的硅质岩中的放射虫化石或蛇绿岩与其他地质体的相互关系来限定其形成的大致时代,随着同位素分析手段的发展,尤其是锆石 U-Pb 定年技术的应用,使地质学家能够更精确的获得蛇绿岩的形成时代。近年来,在内蒙古东南部地区,一些学者先后获得了贺根山蛇绿岩、索伦山蛇绿岩以及达青牧场—迪彦庙蛇绿混杂岩的锆石年龄资料^[18-20, 33-36],为该地区的构造演化研究提供了较为精确的年代学依据。考虑到西拉木伦河蛇绿岩带还缺少精确的锆石年龄报道,本次工作在相关项目的资助下,对位于该蛇绿岩带东段的九井子蛇绿岩及其围岩开展了锆石 U-Pb 定年,试图对它们的形成时代进行约束,并结合前人资料进一步探讨西拉木伦河蛇绿岩带的构造演化及其地质意义。

1 区域地质概况和岩石学特征

西拉木伦河蛇绿岩带大致沿内蒙古东南部的

西拉木伦河北岸呈东西向断续分布,由柯单山、杏树洼(小苇塘)、九井子等蛇绿岩残片构成,岩石类型主要包括蛇纹石化橄榄岩、辉长岩、辉石岩以及变玄武岩,这些蛇绿岩多以孤立的构造块体的形式与古生代浅变质岩系呈构造接触^[15~16,37]。其中,作为西伯利亚和中朝古板块缝合带重要证据之一的中二叠世放射虫硅质岩就产出在杏树洼蛇绿岩片中^[17]。蛇绿岩带南北两侧分别是中朝古陆北部增生边缘和西伯利亚古陆南部面向古亚洲洋的增生边缘^[1]。晚古生代以来,南部的中朝古陆北缘从西拉木伦河蛇绿岩带到阴山—燕山北部的“内蒙地轴”发育强烈的钙碱性系列的岩浆活动,形成了类似安第斯造山带的活动大陆边缘^[38~39]。而北部西伯利亚古陆面向古亚洲洋的增生边缘则形成由众多的岩浆弧、前寒武纪地块、条带状古老洋壳(蛇绿岩)所构成的增生楔^[8~9,40],并广泛发育晚石炭世到晚二叠世以来的海相沉积,其中早二叠世大石寨组主要由火山岩及其碎屑岩组成,中二叠世哲斯组和晚二叠世林西组则主体由海相砂岩、页岩、碳酸盐岩以及板岩组成,直到晚二叠世末才出现陆相沉积地层^[23,41~42]。

本次工作的研究对象,九井子蛇绿岩位于内蒙古巴林左旗南部的九井子村一带,呈北东向不规则椭圆状产出,长约3 km,宽约0.5 km。蛇绿岩南东侧与原定中石炭世碎屑岩呈断层接触,西侧被中生代陆相火山沉积岩系不整合覆盖,北侧被中生代碱长花岗岩侵入,南侧则被第四系黄土所覆盖(图1)。岩石类型主要包括蛇纹岩、辉长岩、玄武岩及硅质粉砂岩。其中,蛇纹岩主要出露在蛇绿岩中西部的采坑和探槽中(图2),岩石呈灰绿色,块状构造,整体发育碎裂变形(图3-a~b);显微镜下岩石主要由纤维状蛇纹石组成,局部保留辉石和橄榄石假象。在蛇绿岩中部的采坑中可见青灰色粉砂岩以及灰黑色泥质粉砂岩,与蛇纹岩呈断层接触(图3-a),其中粉砂岩为块状构造,接触带附近也发生强烈的碎裂变形(图3-c)。辉长岩为浅灰绿色,呈不规则脉状产出在蛇纹岩中,由于侵位过程中岩浆流动,显示弱片麻状构造(图3-d, e)。显微镜下观察,辉长岩主要由斜长石、辉石及角闪石组成,半自形粒状结构;其中,斜长石粒度0.2~1 mm,含量60%~70%,辉石和角闪石粒度较小,0.1~0.5 mm,含量30%~40%。受后期构造变形影响,岩石中发育不规

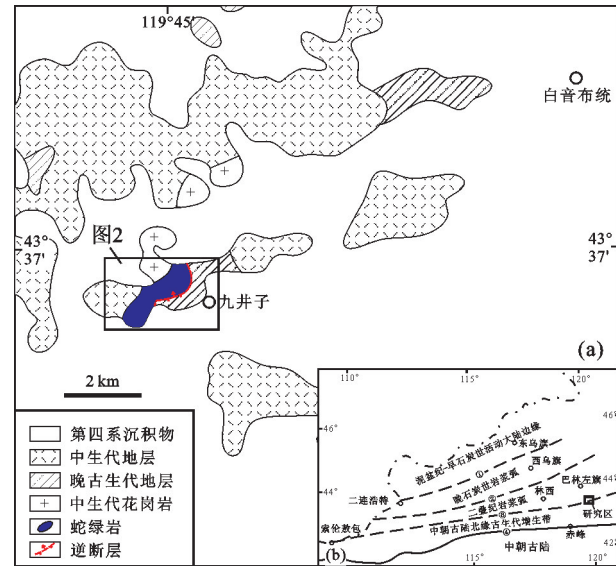


图1 巴林左旗九井子地区地质简图(a)和内蒙古东南部构造分区简图(b,据文献[40])

①—二连浩特—贺根山断裂带;②—锡林浩特—达青牧场断裂带;
③—索伦山—西拉木伦河断裂带;④—赤峰—开原断裂带

Fig.1 Simplified geological map of Jiujingzhi area, Bairin Left Banner (a) and tectonic framework of southeastern Inner Mongolia (b)

①—Erlian Hot—Hegenshan fault zone; ②—Xilin Hot—Daqing Pasture fault zone; ③—Suolunshan—Xar Moron fault zone;
④—Chifeng—Kaiyuan fault zone

则裂隙,沿裂隙发生绿帘石—绿泥石化蚀变(图3-g)。辉长岩中平行片麻理还发育辉长伟晶岩脉,推测为岩浆演化晚期的产物。此外,北东部的采坑中为深灰绿色块状玄武岩及凝灰岩,分别发育粗玄结构和碎屑结构;受后期构造热事件的影响,镁铁质矿物多蚀变为绿帘石和绿泥石。

为了限定九井子蛇绿岩的构造侵位时代,本次工作还对蛇绿岩南东侧采坑中的粉砂岩进行了样品采集和分析测试。粉砂岩为浅灰绿色,风化面为黄褐色,岩石呈块状构造,受构造变形影响发育北东向片理化带(图3-f),且越靠近蛇绿岩变形越强,推测两者应为断层接触。显微镜下观察,岩石主要由石英、长石晶屑组成,粒径50~100 μm,含量30%~35%,由钙质和粉砂质胶结(图3-h)。

2 样品制备和分析方法简介

锆石分选是在河北省廊坊市诚信地质服务公司完成的,先将样品机械粉碎,经磁选和重液淘洗



图2 九井子蛇绿岩卫星影像图(Google Earth 截图, 黄色虚线示意蛇绿岩分布范围)

Fig.2 Satellite image of Jiujingzi ophiolite (Downloaded from Google Earth, the yellow dotted line indicating the distribution area of Jiujingzi ophiolite)

后在双目镜下挑纯。然后,选择透明无包裹体、无裂隙、晶形好的锆石进行年龄样品靶的制备,制备方法与 SHRIMP 方法类似^[43]。将锆石靶镀碳后,进行阴极发光(CL)图像采集,辉长岩和粉砂岩锆石 CL 图像是分别在武汉上谱分析科技有限责任公司 JSM-IT100 扫描电镜和国土资源部大陆构造与动力学重点实验室 Nova Nano SEM 450 场发射扫描电子显微镜上获取的。

锆石定年在吉林大学东北亚矿产资源评价国土资源部重点实验室进行,采用激光剥蚀等离子体质谱分析技术(LA-ICP-MS),应用 COMPExPro 型 ArF 准分子激光剥蚀系统和 Agilent 7900 型 ICP-MS 进行锆石 U-Pb 测定,激光束斑为 32 μm。U-Pb 同位素定年中采用锆石标准 91500 作外标进行同位素分馏校正,详细的实验原理和流程参见文献[44]。对分析数据的离线处理采用软件 ICPMSDataCal^[44-45]完成。锆石样品的 U-Pb 年龄谐和图绘制和年龄权重平均计算采用程序 Isoplot(ver 3.00)^[46]完成。

3 锆石 U-Pb 定年结果

3.1 九井子辉长岩锆石定年结果

为了限定九井子蛇绿岩的形成时代,本次工作

对产出在蛇纹岩中的辉长岩脉开展了锆石 U-Pb 定年。定年样品(DL01-7)位于蛇绿岩南东侧采坑,地理坐标为 43°36'45.7"N, 119°45'08.9"E(图2)。所测锆石均为无色透明粒状或短柱状晶体,粒径 100~150 μm,长宽比多介于 1:1~2:1。从阴极发光图像(图 4-a, b)来看,锆石多发育较宽的生长条纹,显示了基性岩浆岩锆石的特征^[47]。对其中 24 颗锆石进行了分析测试,分析结果表明,所测锆石 Th/U 比介于 0.24~0.47,也反映了岩浆成因锆石的特征(表 1)。在 U-Pb 年龄谐和图中,所有样品点均投影到谐和线上及附近, $^{206}\text{Pb}/^{238}\text{U}$ 年龄加权平均值为 (274.7 ± 1.7) Ma, MSWD=0.079(图 5),表明该辉长岩脉形成于早二叠世晚期。

3.2 晚古生代碎屑岩定年结果

粉砂岩定年样品(DA02-1)采自九井子蛇绿岩南东侧采坑,地理坐标为 43°36'21.4"N, 119°45'04.3"E(图2)。该样品锆石粒度介于 50~200 μm;根据晶体形态,锆石可以进一步划分为较自形的粒状、长柱状晶体和浑圆状晶体两种类型,反映不同来源的特征。在阴极发光图像上(图 4-c, d),较自形的锆石具有清晰的振荡环带以及较强的发光,显示岩浆锆石的特征;而浑圆状锆石显示较弱的发光特征以及较模



图3 九井子蛇绿岩及其围岩野外露头和显微照片

a—蛇纹岩与泥质粉砂岩断层接触; b—灰绿色蛇纹岩; c—浅灰绿色粉砂岩; d—辉长岩中伟晶岩脉; e—辉长岩(DL01-7)野外照片; f—粉砂岩(DA02-1)野外照片; g—辉长岩(DA02-1)显微照片; h—粉砂岩(DA02-1)显微照片; Cpx—单斜辉石; Hb—角闪石; Pl—斜长石

Fig. 3 Field outcrop photograph and microphotographs of Jiujingzi ophiolite and adjacent rocks

a—Fault contact between serpentinite and pelitic siltstone; b—Grayish-green serpentinite; c—Light grayish-green siltstone; d—Gabbro pegmatite in fine-grained gabbro; e—Field photograph of gabbro sample (DL01-7); f—Field photograph of siltstone sample (DA02-1); g—Microphotograph of gabbro sample (DL01-7); h—Microphotograph of siltstone sample (DA02-1); Cpx—Clinopyroxene; Hb—Hornblende; Pl—Plagioclase

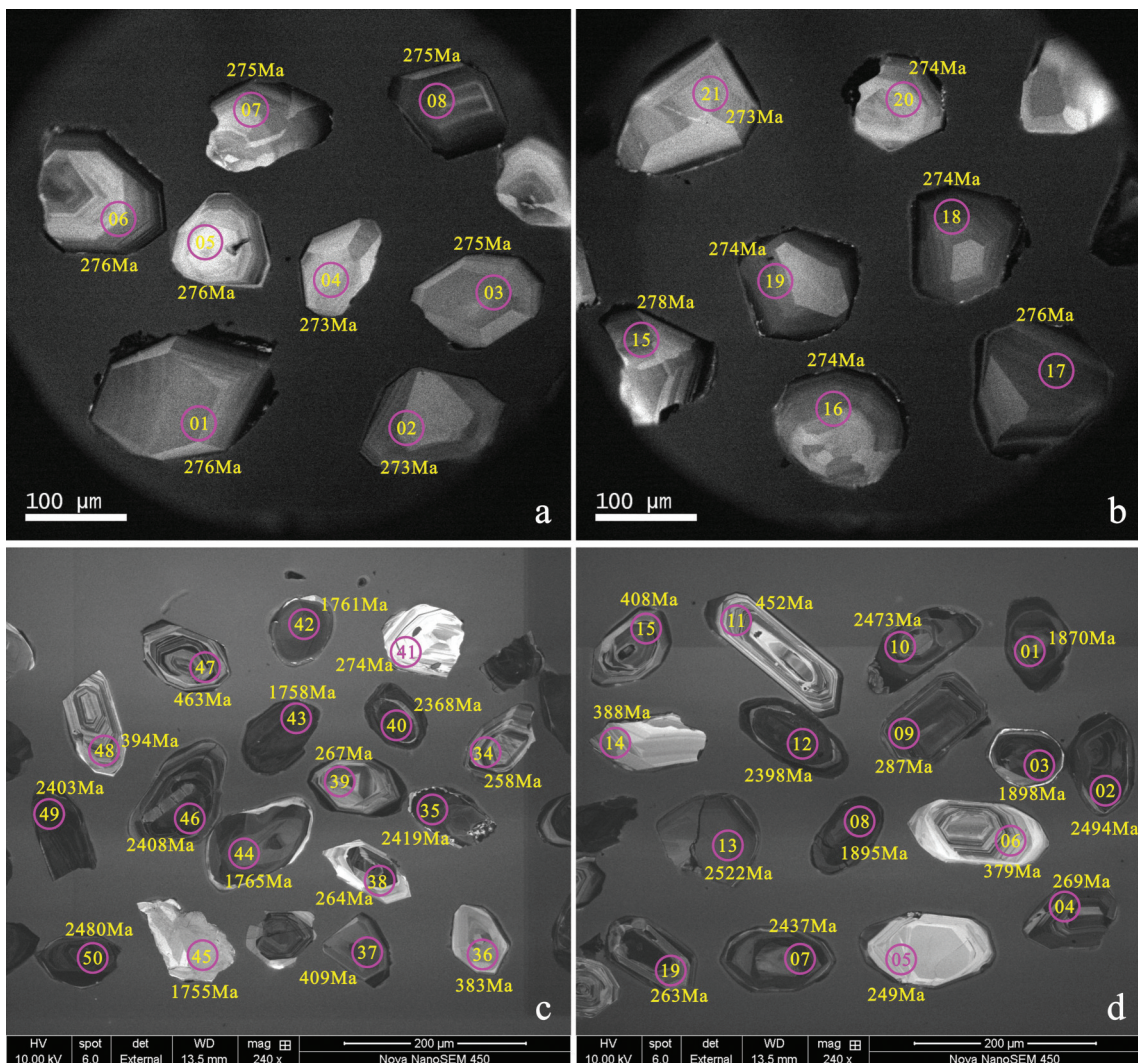


图4 九井子辉长岩脉(DL01-7)锆石(a和b)及粉砂岩(DA02-1)碎屑锆石(c和d)阴极发光图像
Fig. 4 Cathodoluminescence (CL) images of zircons (a and b) from the gabbro dike(DL01-7) of Jiujingzi ophiolite and detrital zircons (c and d) from adjacent siltstone(DA02-1)

糊的内部结构,其中大部分具有明显的核边结构,反映锆石形成后受到了后期构造热事件的改造。

对102颗锆石进行了U-Pb定年,分析结果见表2。除去 $^{206}\text{Pb}/^{238}\text{U}$ 和 $^{207}\text{Pb}/^{235}\text{U}$ 年龄谐和度小于90%的7颗锆石以外,其余95颗锆石的分析结果均分布在谐和线上及附近(图6-a, b)。考虑到年轻锆石(<1000 Ma)放射性成因 ^{207}Pb 含量较少,分析中容易产生较大的误差,在下面的讨论过程中,对于年轻的锆石(<1000 Ma)使用 $^{206}\text{Pb}/^{238}\text{U}$ 年龄,对于较老的锆石(>1000 Ma)使用 $^{206}\text{Pb}/^{207}\text{Pb}$ 年龄。

从统计直方图中,除24(342 Ma)、82(1335 Ma)、83(1050 Ma)和102(1443 Ma)号锆石年龄比较分散外,较谐和的锆石年龄大致构成4个峰值:250~290 Ma、370~470 Ma、1700~2100 Ma和2350~2700 Ma(图6-c),其中第二个年龄峰值可以进一步划分为370~420 Ma和450~470 Ma两个次级峰(图6-d)。在阴极发光图像上,显生宙以来的锆石多显示较好的晶形和清晰的环带,而元古宙和太古宙的锆石则对应发光较弱的浑圆状晶体(图4-c, d)。上述定年结果表明,该粉砂岩应形成于晚二叠世末—

表1 九井子蛇绿岩辉长岩脉(DL01-7)锆石LA-ICPMS U-Pb测年结果
Table 1 Zircon LA-ICPMS U-Pb dating result of the gabbro dike (DL01-7) in Jiujingzi ophiolite

点号	含量/ $\mu\text{g/g}^{-1}$		$^{232}\text{Th}/^{238}\text{U}$		$^{207}\text{Pb}/^{206}\text{Pb}$		$^{207}\text{Pb}/^{235}\text{U}$		$^{206}\text{Pb}/^{238}\text{U}$		$^{208}\text{Pb}/^{232}\text{Th}$		$^{207}\text{Pb}/^{206}\text{Pb}$		$^{207}\text{Pb}/^{235}\text{U}$		$^{206}\text{Pb}/^{238}\text{U}$		$^{208}\text{Pb}/^{232}\text{Th}$	
	Pb	^{232}Th	^{238}U	$^{207}\text{Pb}/^{206}\text{Pb}$	$\pm 1\sigma$	$^{207}\text{Pb}/^{235}\text{U}$	$\pm 1\sigma$	$^{206}\text{Pb}/^{238}\text{U}$	$\pm 1\sigma$	$^{208}\text{Pb}/^{232}\text{Th}$	$\pm 1\sigma$	$^{207}\text{Pb}/^{206}\text{Pb}$	$\pm 1\sigma$	$^{207}\text{Pb}/^{235}\text{U}$	$\pm 1\sigma$	$^{206}\text{Pb}/^{238}\text{U}$	$\pm 1\sigma$	$^{208}\text{Pb}/^{232}\text{Th}$	$\pm 1\sigma$	
01	3.0	18	55	0.33	0.0518	0.0026	0.3156	0.0159	0.0438	0.0008	0.0138	0.0005	276	108.3	279	12.3	276	4.9	278	10.2
02	2.3	11	43	0.26	0.0509	0.0047	0.3040	0.0281	0.0433	0.0009	0.0126	0.0009	235	21.3	270	21.9	273	5.4	254	18.9
03	2.3	15	41	0.37	0.0524	0.0031	0.3139	0.0182	0.0435	0.0007	0.0136	0.0005	306	137	277	14.1	275	4.2	273	10.0
04	2.9	14	53	0.27	0.0522	0.0020	0.3125	0.0117	0.0433	0.0006	0.0136	0.0005	295	90	276	9.1	273	3.8	273	9.5
05	2.4	12	43	0.28	0.0517	0.0032	0.3107	0.0193	0.0437	0.0008	0.0138	0.0008	333	144	275	14.9	276	4.7	277	16.8
06	4.1	18	75	0.24	0.0502	0.0023	0.3050	0.0148	0.0437	0.0007	0.0130	0.0006	206	107.4	270	11.5	276	4.1	260	11.5
07	3.9	20	76	0.26	0.0524	0.0024	0.3155	0.0140	0.0436	0.0008	0.0141	0.0005	302	106	278	10.8	275	4.7	284	10.4
08	5.2	42	90	0.47	0.0524	0.0019	0.3144	0.0115	0.0436	0.0006	0.0135	0.0004	302	81.5	278	8.9	275	3.8	271	7.1
09	2.1	11	39	0.29	0.0525	0.0029	0.3157	0.0173	0.0436	0.0008	0.0141	0.0008	306	129	279	13.3	275	4.9	284	16.9
10	4.9	27	88	0.30	0.0526	0.0024	0.3180	0.0150	0.0436	0.0007	0.0142	0.0004	322	101	280	11.6	275	4.2	284	7.8
11	4.6	37	79	0.47	0.0523	0.0020	0.3142	0.0119	0.0435	0.0007	0.0136	0.0003	298	89.8	277	9.2	275	4.0	274	6.7
12	4.2	31	74	0.43	0.0522	0.0021	0.3110	0.0125	0.0434	0.0006	0.0135	0.0004	295	94.4	275	9.7	274	3.5	271	7.7
13	4.7	31	85	0.37	0.0498	0.0025	0.2949	0.0136	0.0433	0.0006	0.0129	0.0005	187	117	262	10.7	273	4.0	260	9.0
14	4.5	33	81	0.41	0.0530	0.0022	0.3161	0.0127	0.0435	0.0006	0.0138	0.0003	328	96.3	279	9.8	274	3.5	276	6.7
15	4.7	22	86	0.26	0.0492	0.0020	0.2993	0.0124	0.0440	0.0006	0.0138	0.0004	167	96.3	266	9.7	278	3.5	276	8.6
16	5.0	26	91	0.28	0.0540	0.0017	0.3226	0.0105	0.0434	0.0005	0.0142	0.0004	369	70.4	284	8.1	274	3.3	286	8.5
17	4.6	37	80	0.46	0.0512	0.0024	0.3120	0.0149	0.0437	0.0006	0.0143	0.0004	250	11.4	276	11.5	276	4.0	286	8.3
18	5.1	24	97	0.25	0.0519	0.0021	0.3157	0.0132	0.0434	0.0007	0.0136	0.0005	283	90.7	279	10.2	274	4.3	273	9.4
19	4.0	20	77	0.25	0.0526	0.0024	0.3160	0.0154	0.0434	0.0008	0.0130	0.0006	322	101.8	279	11.9	274	5.2	261	11.3
20	2.4	12	46	0.26	0.0527	0.0030	0.3166	0.0181	0.0435	0.0009	0.0125	0.0007	322	125	279	14.0	274	5.3	251	14.8
21	1.9	10	35	0.29	0.0531	0.0028	0.3137	0.0164	0.0433	0.0007	0.0130	0.0006	332	123	277	12.7	273	4.3	261	12.3
22	3.0	25	53	0.47	0.0526	0.0023	0.3158	0.0137	0.0435	0.0007	0.0136	0.0004	309	98.1	279	10.6	274	4.0	273	7.8
23	2.2	16	40	0.39	0.0537	0.0024	0.3157	0.0125	0.0433	0.0007	0.0133	0.0005	367	101.8	279	10.5	273	4.2	267	10.0
24	3.1	16	57	0.27	0.0543	0.0025	0.3239	0.0146	0.0436	0.0006	0.0167	0.0008	387	102	285	11.2	275	4.0	336	15.1

表2 九井子蛇绿岩南东侧粉砂岩(DA02-1)碎屑锆石LA-ICPMS U-Pb测年结果
 Table 2 LA-ICPMS U-Pb dating results of detrital zircons from the siltstone(DA02-1) on the southeast side of Jujingzi ophiolite

点号	含量/ $\mu\text{g g}^{-1}$		同位素比值						年龄/Ma											
	Pb	^{232}Th	^{238}U	$^{232}\text{Th}/^{238}\text{U}$	$^{207}\text{Pb}/^{206}\text{Pb}$	$\pm 1\sigma$	$^{207}\text{Pb}/^{235}\text{U}$	$\pm 1\sigma$	$^{208}\text{Pb}/^{232}\text{Th}$	$\pm 1\sigma$	$^{207}\text{Pb}/^{235}\text{U}$	$\pm 1\sigma$	$^{206}\text{Pb}/^{238}\text{U}$	$\pm 1\sigma$	$^{208}\text{Pb}/^{232}\text{Th}$	$\pm 1\sigma$				
01	188	774	1016	0.76	0.1144	0.0032	2.3262	0.0675	0.1460	0.0021	0.0300	0.0010	1870	51	1220	21	878	12	598	20
02	190	217	305	0.71	0.1636	0.0042	10.6600	0.2736	0.4656	0.0044	0.1338	0.0040	2494	43	2494	24	2464	19	2574	72
03	159	218	410	0.53	0.1162	0.0029	4.8645	0.1251	0.3008	0.0035	0.0911	0.0027	1898	46	1796	22	1696	18	1763	50
04	17	334	302	1.11	0.0512	0.0027	0.3034	0.0159	0.0426	0.0006	0.0139	0.0004	254	122	269	12	269	4	280	9
05	3	33	64	0.52	0.0531	0.0071	0.2802	0.0356	0.0394	0.0008	0.0130	0.0010	332	278	251	28	249	5	262	20
06	15	152	197	0.77	0.0536	0.0030	0.4544	0.0253	0.0606	0.0010	0.0195	0.0008	354	126	380	18	379	6	391	15
07	164	125	293	0.43	0.1582	0.0045	9.9349	0.2689	0.4493	0.0054	0.1232	0.0042	2437	48	2429	25	2392	24	2348	76
08	124	55	334	0.16	0.1160	0.0030	5.2344	0.1309	0.3223	0.0035	0.0939	0.0030	1895	47	1858	21	1801	17	1814	56
09	29	262	541	0.48	0.0515	0.0020	0.3276	0.0131	0.0455	0.0006	0.0150	0.0005	261	91	288	10	287	4	301	10
10	135	129	219	0.59	0.1616	0.0038	10.6598	0.2507	0.4719	0.0050	0.1245	0.0036	2473	45	2494	22	2492	22	2371	64
11	17	80	196	0.41	0.0559	0.0023	0.5660	0.0233	0.0727	0.0009	0.0198	0.0008	450	86	455	15	452	5	396	15
12	112	140	210	0.67	0.1546	0.0047	8.5155	0.2769	0.3968	0.0072	0.1113	0.0039	2398	52	2288	30	2154	33	2133	71
13	49	41	84	0.49	0.1654	0.0049	10.4266	0.3067	0.4534	0.0058	0.1128	0.0040	2522	50	2473	27	2410	26	2161	74
14	6	24	76	0.32	0.0549	0.0041	0.4648	0.0336	0.0620	0.0010	0.0206	0.0015	409	165	388	23	388	6	412	29
15	25	218	291	0.75	0.0554	0.0023	0.5023	0.0201	0.0654	0.0009	0.0188	0.0006	428	86	413	14	408	5	376	12
16	152	181	79	0.1641	0.0041	10.6716	0.2757	0.4660	0.0056	0.1233	0.0039	2498	42	2495	24	2466	25	2351	70	
17	192	235	393	0.60	0.1582	0.0045	7.7867	0.2263	0.3505	0.0045	0.0907	0.0032	2437	49	2207	26	1937	21	1756	60
18	14	65	181	0.36	0.0544	0.0027	0.4708	0.0234	0.0625	0.0009	0.0169	0.0008	387	113	392	16	391	5	339	17
19	21	236	400	0.59	0.0511	0.0027	0.2935	0.0150	0.0416	0.0006	0.0127	0.0006	256	120	261	12	263	4	255	12
20	14	141	174	0.81	0.0536	0.0025	0.4383	0.0200	0.0591	0.0008	0.0170	0.0007	354	99	369	14	370	5	340	13
21	18	203	342	0.59	0.0523	0.0022	0.2992	0.0122	0.0408	0.0005	0.0119	0.0004	298	96	263	10	258	3	239	9
22	23	123	245	0.50	0.0560	0.0021	0.5757	0.0209	0.0739	0.0009	0.0219	0.0008	454	81	462	13	460	6	437	16
23	42	61	70	0.1860	0.0054	12.4435	0.3609	0.4791	0.0063	0.1200	0.0042	2707	48	2638	27	2523	28	2291	75	
24	21	318	264	1.21	0.0534	0.0023	0.4037	0.0168	0.0545	0.0007	0.0158	0.0006	343	92	346	12	342	5	316	11
25	153	236	231	1.02	0.1725	0.0054	10.6510	0.3272	0.4395	0.0049	0.1106	0.0042	2583	54	2493	29	2349	22	2119	77

续表2

点号	含量/ $\mu\text{g}\cdot\text{g}^{-1}$			同位素比值						年龄/Ma				
	Pb	^{232}Th	^{238}U	$^{232}\text{Th}/^{238}\text{U}$	$^{207}\text{Pb}/^{206}\text{Pb}$	$\pm 1\sigma$	$^{207}\text{Pb}/^{235}\text{U}$	$\pm 1\sigma$	$^{206}\text{Pb}/^{238}\text{U}$	$\pm 1\sigma$	$^{207}\text{Pb}/^{232}\text{Th}$	$\pm 1\sigma$	$^{206}\text{Pb}/^{238}\text{U}$	$\pm 1\sigma$
26	49	354	582	0.61	0.0593	0.0019	0.5485	0.0170	0.0659	0.0008	0.0198	0.0007	589	72
27	58	119	80	1.48	0.1695	0.0049	10.5262	0.3021	0.4488	0.0052	0.1120	0.0035	2553	53
28	103	118	273	0.43	0.1196	0.0031	4.9304	0.1307	0.2968	0.0034	0.0769	0.0026	1950	46
29	11	139	213	0.65	0.0519	0.0030	0.2848	0.0156	0.0400	0.0006	0.0108	0.0005	280	133
30	151	46	388	0.12	0.1180	0.0035	5.4009	0.1657	0.3505	0.0041	0.0947	0.0037	1926	58
31	167	200	319	0.63	0.1586	0.0047	8.1394	0.2553	0.3692	0.0048	0.1176	0.0044	2443	50
32	239	187	408	0.46	0.1720	0.0046	10.0987	0.2785	0.4234	0.0048	0.1120	0.0037	2577	44
33	135	200	205	0.98	0.1548	0.0039	9.7292	0.2550	0.4530	0.0055	0.1219	0.0039	2399	38
34	11	156	212	0.74	0.0569	0.0030	0.2857	0.0164	0.0498	0.0006	0.0113	0.0004	239	133
35	205	260	327	0.79	0.1566	0.0041	9.4660	0.2600	0.4365	0.0048	0.1183	0.0042	2419	44
36	9	59	110	0.54	0.0528	0.0035	0.4543	0.0293	0.0611	0.0009	0.0202	0.0010	320	150
37	20	166	228	0.73	0.0545	0.0023	0.4970	0.0216	0.0656	0.0009	0.0208	0.0009	394	96
38	25	516	367	1.41	0.0514	0.0023	0.2952	0.0130	0.0418	0.0006	0.0152	0.0006	257	106
39	10	148	167	0.89	0.0517	0.0028	0.3008	0.0163	0.0423	0.0006	0.0129	0.0005	272	124
40	180	118	298	0.40	0.1520	0.0036	9.5079	0.2260	0.4516	0.0047	0.1407	0.0043	2368	41
41	4	45	76	0.59	0.0535	0.0079	0.3126	0.0452	0.0435	0.0010	0.0150	0.0010	350	304
42	96	66	241	0.27	0.1076	0.0029	4.7394	0.1284	0.3181	0.0039	0.0968	0.0033	1761	49
43	141	261	309	0.84	0.1075	0.0029	4.7784	0.1302	0.3193	0.0039	0.0983	0.0032	1758	49
44	68	81	177	0.46	0.1078	0.0028	4.3608	0.1099	0.2917	0.0031	0.0815	0.0024	1765	46
45	23	43	64	0.67	0.1074	0.0032	3.9517	0.1199	0.2646	0.0033	0.0750	0.0024	1755	55
46	292	377	463	0.81	0.1556	0.0033	9.4428	0.2068	0.4370	0.0047	0.1161	0.0032	2408	42
47	30	208	309	0.67	0.0564	0.0018	0.5795	0.0181	0.0745	0.0010	0.0230	0.0007	465	74
48	14	117	172	0.68	0.0545	0.0023	0.4775	0.0211	0.0631	0.0008	0.0194	0.0007	394	96
49	268	161	531	0.30	0.1551	0.0041	8.5253	0.2280	0.3969	0.0059	0.1069	0.0040	2403	45
50	195	210	311	0.68	0.1621	0.0038	10.2177	0.2434	0.4528	0.0046	0.1193	0.0035	2480	39
51	11	93	224	0.42	0.0509	0.0026	0.2972	0.0146	0.0424	0.0006	0.0119	0.0005	235	114

续表2

点号	同位素比值										年龄/Ma									
	Pb	^{232}Th	^{238}U	$^{232}\text{Th}/^{238}\text{U}$	$^{207}\text{Pb}/^{206}\text{Pb}$	$\pm 1\sigma$	$^{207}\text{Pb}/^{235}\text{U}$	$\pm 1\sigma$	$^{208}\text{Pb}/^{232}\text{Th}$	$\pm 1\sigma$	$^{207}\text{Pb}/^{206}\text{Pb}$	$\pm 1\sigma$	$^{208}\text{Pb}/^{235}\text{U}$	$\pm 1\sigma$	$^{207}\text{Pb}/^{238}\text{U}$	$\pm 1\sigma$	$^{206}\text{Pb}/^{238}\text{U}$	$\pm 1\sigma$	$^{207}\text{Pb}/^{232}\text{Th}$	$\pm 1\sigma$
52	90	104	177	0.59	0.1302	0.0031	6.9253	0.1680	0.3818	0.0041	0.0981	0.0026	2102	42	2102	22	2085	19	1891	48
53	78	84	123	0.68	0.1603	0.0040	10.2387	0.2589	0.4581	0.0048	0.1204	0.0033	2459	43	2457	23	2431	21	2298	60
54	17	70	198	0.35	0.0557	0.0024	0.5689	0.0246	0.0739	0.0010	0.0218	0.0009	439	131	457	16	460	6	435	19
55	207	273	341	0.80	0.1619	0.0044	9.9523	0.2818	0.4407	0.0060	0.1117	0.0034	2476	46	2430	26	2354	27	2141	62
56	19	85	212	0.40	0.0561	0.0028	0.5855	0.0274	0.0751	0.0011	0.0229	0.0009	457	111	468	18	467	6	457	18
57	383	117	1229	0.10	0.1050	0.0024	3.8490	0.0882	0.2630	0.0027	0.0801	0.0022	1714	41	1603	18	1505	14	1557	41
58	10	60	103	0.58	0.0568	0.0031	0.5754	0.0307	0.0738	0.0011	0.0228	0.0010	487	122	461	20	459	7	457	19
59	18	268	323	0.83	0.0517	0.0022	0.2922	0.0119	0.0408	0.0004	0.0127	0.0004	333	98	260	9	258	3	255	8
60	207	137	341	0.40	0.1606	0.0043	10.2718	0.2669	0.4593	0.0047	0.1347	0.0046	2462	45	2460	24	2437	21	2555	82
61	117	163	242	0.67	0.1634	0.0046	7.9571	0.2213	0.3504	0.0046	0.0859	0.0033	2491	48	2226	25	1936	22	1665	62
62	200	42	633	0.07	0.1403	0.0035	5.1337	0.1354	0.2621	0.0034	0.0544	0.0022	2231	43	1842	22	1501	18	1071	41
63	58	85	92	0.93	0.1662	0.0041	10.0829	0.2382	0.4351	0.0045	0.1190	0.0035	2519	41	2442	22	2328	20	2273	63
64	164	153	273	0.56	0.1638	0.0037	10.4192	0.2334	0.4516	0.0046	0.1181	0.0033	2516	37	2473	21	2402	20	2257	60
65	26	348	352	0.99	0.0653	0.0027	0.4725	0.0198	0.0518	0.0007	0.0179	0.0006	783	86	393	14	326	4	358	11
66	88	102	133	0.76	0.1695	0.0043	11.3175	0.2962	0.4781	0.0052	0.1267	0.0036	2553	43	2550	24	2519	23	2411	64
67	77	134	175	0.76	0.1122	0.0030	5.2046	0.1364	0.3345	0.0032	0.0909	0.0025	1835	49	1853	22	1860	15	1759	47
68	87	115	175	0.65	0.1287	0.0032	6.5531	0.1618	0.3664	0.0036	0.1007	0.0028	2081	44	2053	22	2012	17	1939	51
69	204	212	492	0.43	0.1140	0.0027	5.2584	0.1253	0.3313	0.0031	0.0855	0.0022	1865	43	1862	20	1845	15	1659	42
70	32	184	346	0.53	0.0548	0.0021	0.5494	0.0206	0.0719	0.0008	0.0222	0.0007	467	82	445	14	448	5	444	14
71	113	132	176	0.75	0.1646	0.0044	10.4558	0.2936	0.4570	0.0052	0.1214	0.0036	2506	46	2476	26	2426	23	2315	64
72	61	99	91	1.09	0.1643	0.0049	10.2699	0.3127	0.4491	0.0055	0.1193	0.0038	2502	50	2459	28	2391	25	2278	69
73	100	89	163	0.55	0.1622	0.0045	10.1608	0.3004	0.4497	0.0057	0.1223	0.0041	2480	47	2450	27	2394	26	2350	73
74	106	82	252	0.32	0.1122	0.0028	5.2197	0.1374	0.3344	0.0039	0.0968	0.0028	1835	46	1856	22	1860	19	1867	52
75	88	105	219	0.48	0.1134	0.0027	4.8861	0.1164	0.3101	0.0029	0.0863	0.0024	1855	43	1800	20	1741	14	1673	44
76	138	119	255	0.47	0.1524	0.0033	8.2818	0.2209	0.3912	0.0061	0.0995	0.0034	2373	37	2262	24	2128	28	1918	62
77	10	92	195	0.47	0.0511	0.0027	0.2948	0.0157	0.0410	0.0005	0.0122	0.0005	243	122	262	12	259	3	246	10

续表2

点号	含量/ $\mu\text{g}\cdot\text{g}^{-1}$		同位素比值						年龄/Ma											
	Pb	^{232}Th	^{238}U	$^{232}\text{Th}/^{238}\text{U}$	$^{207}\text{Pb}/^{206}\text{Pb}$	$\pm 1\sigma$	$^{206}\text{Pb}/^{238}\text{U}$	$\pm 1\sigma$	$^{208}\text{Pb}/^{232}\text{Th}$	$\pm 1\sigma$	$^{207}\text{Pb}/^{206}\text{Pb}$	$\pm 1\sigma$	$^{207}\text{Pb}/^{235}\text{U}$	$\pm 1\sigma$	$^{208}\text{Pb}/^{238}\text{U}$	$\pm 1\sigma$	$^{208}\text{Pb}/^{232}\text{Th}$	$\pm 1\sigma$		
78	137	166	206	0.80	0.1669	0.0039	10.4739	0.2890	0.4707	0.0074	0.1327	0.0044	2466	41	2478	26	2487	33	2518	78
79	43	42	68	0.61	0.1730	0.0044	10.5920	0.2806	0.4435	0.0054	0.1225	0.0041	2587	43	2488	25	2366	24	2336	74
80	169	150	277	0.54	0.1636	0.0035	10.0631	0.2203	0.4469	0.0049	0.1141	0.0031	2494	36	2441	20	2382	22	2183	56
81	14	61	163	0.37	0.0559	0.0025	0.5551	0.0242	0.0720	0.0010	0.0215	0.0009	456	98	448	16	448	6	430	17
82	256	201	1039	0.19	0.0859	0.0019	2.4862	0.0569	0.2094	0.0023	0.0712	0.0022	1335	41	1268	17	1226	12	1391	42
83	51	51	262	0.19	0.0743	0.0019	1.7280	0.0450	0.1683	0.0018	0.0449	0.0013	1050	52	1019	17	1003	10	887	26
84	66	70	104	0.68	0.1650	0.0043	10.3518	0.2774	0.4541	0.0050	0.1138	0.0033	2507	44	2467	25	2413	22	2178	59
85	134	110	214	0.52	0.1679	0.0039	10.7548	0.2611	0.4631	0.0047	0.1241	0.0033	2539	39	2502	23	2453	21	2365	60
86	12	102	129	0.79	0.0553	0.0028	0.5033	0.0253	0.0661	0.0009	0.0195	0.0006	433	113	414	17	413	5	390	12
87	121	93	314	0.30	0.1127	0.0025	4.8557	0.1085	0.3120	0.0030	0.0867	0.0024	1843	41	1795	19	1751	15	1680	45
88	86	81	138	0.59	0.1660	0.0039	10.3628	0.2486	0.4516	0.0051	0.1253	0.0037	2518	39	2468	22	2402	22	2386	67
89	98	67	240	0.28	0.1159	0.0029	5.2809	0.1378	0.3294	0.0034	0.0970	0.0032	1894	46	1866	22	1836	17	1871	59
90	65	48	123	0.39	0.1635	0.0046	9.0252	0.2557	0.3995	0.0045	0.1133	0.0042	2492	48	2341	26	2167	21	2170	77
91	12	176	192	0.92	0.0527	0.0030	0.3117	0.0172	0.0433	0.0006	0.0140	0.0005	317	128	276	13	273	4	280	11
92	97	169	214	0.79	0.1138	0.0029	5.1049	0.1333	0.3244	0.0033	0.0926	0.0030	1861	46	1837	22	1811	16	1789	55
93	119	142	186	0.76	0.1603	0.0037	10.0268	0.2470	0.4519	0.0046	0.1229	0.0040	2459	38	2437	23	2404	21	2344	72
94	8	98	85	1.15	0.0555	0.0037	0.4881	0.0320	0.0646	0.0010	0.0198	0.0008	432	148	404	22	403	6	397	15
95	145	234	272	0.86	0.1223	0.0031	6.2886	0.1728	0.3715	0.0038	0.1080	0.0038	1991	46	2017	24	2037	18	2073	69
96	20	170	233	0.73	0.0553	0.0025	0.4847	0.0222	0.0638	0.0009	0.0178	0.0008	433	100	401	15	399	6	356	15
97	69	70	115	0.61	0.1655	0.0049	10.0486	0.3154	0.4390	0.0050	0.1037	0.0043	2513	50	2439	29	2346	22	1994	79
98	139	138	214	0.64	0.1810	0.0047	11.5985	0.3221	0.4621	0.0047	0.1074	0.0039	2661	44	2573	26	2449	21	2062	72
99	160	63	459	0.14	0.1102	0.0028	4.4998	0.1228	0.2941	0.0031	0.0746	0.0027	1802	48	1731	23	1662	15	1454	51
100	217	74	1457	0.05	0.1005	0.0028	1.7733	0.0504	0.1272	0.0014	0.0499	0.0022	1633	52	1036	18	772	8	985	43
101	16	159	288	0.55	0.0527	0.0025	0.3272	0.0152	0.0449	0.0005	0.0150	0.0005	322	103	287	12	283	3	260	11
102	108	296	314	0.94	0.0908	0.0032	3.0622	0.1049	0.2426	0.0027	0.0624	0.0025	1443	66	1423	26	1400	14	1223	48

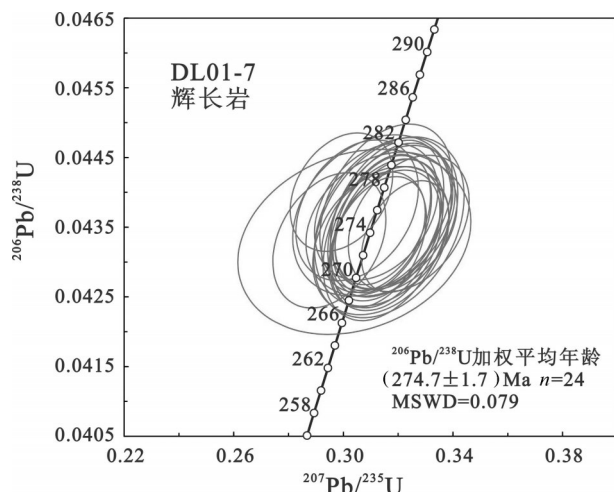


图5 九井子辉长岩脉锆石U-Pb年龄谐和图

Fig. 5 Zircon U - Pb concordia diagram of the gabbro dike in Jiujingzi ophiolite

早三叠世初,其物源既有显生宙以来的地壳物质,也有元古宙和太古宙的物质成分。

4 地质意义讨论

4.1 西拉木伦河蛇绿岩带的形成时代

对于西拉木伦河蛇绿岩的形成时代,一些学者曾在柯单山硅质岩和石灰岩中发现奥陶纪薄壳型介形虫化石 *Ectoprimitia* sp. 以及早古生代早期的 *Asteropylorus cruciporus* Wang (MS) 和 *Pylosphaera* sp. 等微体化石^[15-16, 48]; 同位素年代学方面,陈森煌等(1991)^[49]获得柯单山蛇绿岩全岩 Sm-Nd 等时线年龄为 (665±46) Ma, 据此上述作者认为柯单山蛇绿岩的形成时代应不晚于奥陶纪。另一方面,王玉净和樊志勇(1997)^[17]在杏树洼蛇绿岩中发现中二叠世中、晚期放射虫化石,被作为西拉木伦河蛇绿岩带形成于中二叠世的一个重要证据。前人对放射虫的研究表明,它是一种正常盐度下的广海浮游微体生物,可以生活在海洋的各个深度,其死后可以埋藏于海洋的不同深度,从远洋深海海底到浅海区^[50-51]。近年来,一些学者依据内蒙古毛登牧场地区中二叠世哲斯组含放射虫化石的层位中发现宏体螺类化石,提出兴蒙造山带内二叠纪放射虫化石可能并非代表深海远洋环境^[31, 52]。

蛇绿岩是大洋岩石圈的残留,是古大洋存在的

直接证据。从九井子蛇绿岩中辉长岩的产出情况来看,早二叠世晚期(274.7±1.7 Ma)还有镁铁质岩浆从地幔中分异出来。另外,近年来1:25万林西县幅区域地质调查对柯单山蛇绿岩中辉长岩脉的锆石定年结果也为中二叠世(281.0±6.4 Ma)^[1],这指示古亚洲洋在早二叠世晚期可能还存在洋脊扩张。另一方面,代表深海沉积环境的放射虫一般产于硅质岩中^[53-55],尽管在中二叠世的浅海相和滨浅海相哲斯组中发现了放射虫化石^[52],而杏树洼蛇绿岩中的放射虫化石正是在硅质岩中发现的^[17],也指示内蒙古东南部在该时期存在深海洋盆。已有的研究表明,古亚洲洋的演化历史是从新元古代开始的^[1-2, 12],前人在柯单山蛇绿岩中发现的奥陶纪微体化石则可能记录了该大洋早期的演化历史。综合上述资料,笔者认为西拉木伦河蛇绿岩带可能代表一个从奥陶纪之前到早二叠世末长期演化的宽广的洋盆。

4.2 九井子蛇绿岩构造侵位时代及地质意义

西拉木伦河蛇绿岩多以孤立的构造块体的形式与古生代浅变质岩呈构造接触,王荃(1986)^[15]依据区域上晚志留世下石碑组与下伏层位的不整合关系,认为蛇绿岩的侵位时代在晚志留世之前。然而,李锦铁等(2007)^[37]对西拉木伦河附近原定古元古代“宝音图群”(或奥陶—志留纪地层)和志留纪地层的研究表明,该地区的“宝音图群”实际上是一套变质比较深的长英质岩石,形成时代为二叠纪,志留纪地层则是包含了不同成因和时代岩块的混杂岩,其中就包括含有二叠纪放射虫硅质岩的杏树洼蛇绿岩岩块;它们共同构成中朝和西伯利亚古板块之间二叠纪中晚期—三叠纪中期的增生碰撞杂岩。

九井子蛇绿岩与其南东侧的粉砂岩呈断层接触,通过对粉砂岩碎屑锆石的分析可以揭示其物源并对蛇绿岩构造侵位的时限进行约束。对于粉砂岩的物源,由于西拉木伦河蛇绿岩带两侧均发育二叠纪岩浆活动^[38-39, 56-57],我们暂无法判定最小的年龄峰值(250~290 Ma)的锆石源区,但是它具有明显的太古宙(2350~2700 Ma)和元古宙(1700~2100 Ma)两个年龄峰值,锆石数量为56颗,占所分析锆石的一半以上,指示华北克拉通前寒武纪基底应是粉砂岩的一个重要源区。另外,中—晚奥陶世(450~470 Ma)和晚志留世—泥盆纪(370~420 Ma)两个年龄

^①中国地质大学(武汉)地质调查研究院. 林西县幅(K50C001003)区域地质调查报告[R].2007.

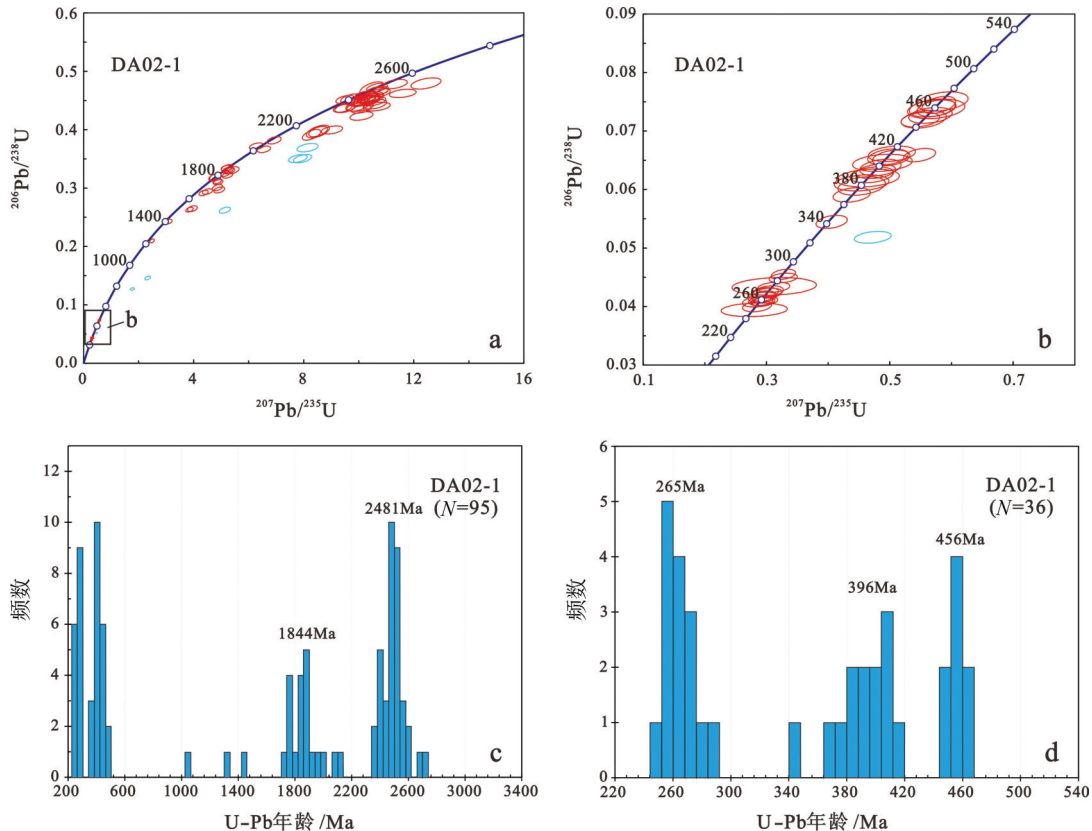


图6 九井子蛇绿岩南东侧晚古生代粉砂岩锆石U-Pb年龄谐和图和统计直方图

Fig. 6 U-Pb concordia diagrams and histograms of zircons of Late Paleozoic siltstone on the southeast side of Jiujingzi ophiolite

峰值的时限大致与白乃庙弧的形成时代及其碰撞增生到华北克拉通北缘的时间一致^[1, 19, 58-60], 这些锆石也应来自中朝古板块早古生代的增生边缘。因此, 粉砂岩的源区应主要来自中朝古陆北缘, 即九井子蛇绿岩侵位过程中是仰冲到中朝古陆北缘之上的。粉砂岩中最小的锆石年龄为(249±4.7) Ma, 属于晚二叠世末—早三叠世初, 该时代与内蒙古东南部海相地层消失的时代^[23, 41-42, 61]、安加拉植物群和华夏植物群出现混生的时代^[21]、西伯利亚和中朝古板块古纬度曲线收敛的时代^[24]以及区域上与碰撞相关岩浆岩的形成时代^[37, 62-63]大致相同。由此, 本文推断九井子蛇绿岩的就位时代也应为晚二叠世末—早三叠世初, 同时可能预示着以西拉木伦蛇绿岩带代表的古亚洲洋的最终闭合。

5 结 论

(1) 西拉木伦河蛇绿岩形成于中二叠世之前, 代表一个从奥陶纪之前到早二叠世长期演化的宽广的洋盆。

(2) 九井子蛇绿岩的构造侵位时代为晚二叠世末—早三叠世初, 可能预示着以西拉木伦蛇绿岩带代表的古亚洲洋的最终闭合。

致谢:笔者野外工作期间得到了中国地质科学院地质研究所张义平和张北航同学的协助, 国土资源部大陆构造与动力学重点实验室施彬博士在锆石阴极发光照相过程中给予的帮助以及中国地质科学院地质研究所李朋武研究员在古地磁学方面给予的指导和帮助, 在此一并致以衷心感谢。

参考文献(References):

- [1] 李锦轶, 张进, 杨天南, 等. 北亚造山区南部及其毗邻地区地壳构造分区与构造演化[J]. 吉林大学学报(地球科学版), 2009, 39(4): 584-605.
Li Jinyi, Zhang Jin, Yang Tiannan, et al. Crustal tectonic division and evolution of the southern part of the north Asian Orogenic region and its adjacent areas [J]. Journal of Jilin University (Earth Science Edition), 2009, 39(4): 584-605 (in Chinese with English abstract).
- [2] Sengör A M C, Natal' in B A, Burtman V S. Evolution of the Altaiid tectonic collage and Paleozoic crustal growth in Eurasia [J].

- Nature, 1993, 364: 209–307.
- [3] Sengör A M C, Natal' in B A. Paleotectonics of Asia: fragments of a synthesis [C]//Yin A, Harrison M (eds.). *The Tectonic Evolution of Asia*. Cambridge: Cambridge University Press, 1996: 486–640.
- [4] Jahn B M, Wu F Y, Hong D W. Important crustal growth in the Phanerozoic: Isotopic evidence of granitoids from East central Asia [J]. *Journal of Earth System Science*, 2000, 109: 5–20.
- [5] Jahn B M, Wu F Y, Chen B. Massive granitoid generation in Central Asia: Nd isotope evidence and implication for continental growth in the Phanerozoic [J]. *Episodes*, 2000b, 23: 82–92.
- [6] Jahn B M, Capdevila R, Liu D Y, et al. Sources of Phanerozoic granitoids in the transect Bayanhongor–Ulaan Baatar, Mongolia: Geochemical and Nd isotopic evidence, and implications for Phanerozoic crustal growth [J]. *Journal of Asian Earth Sciences*, 2004, 23: 629–653.
- [7] Badarch G, Cunningham W D, Windley B F. A new terrane subdivision for Mongolia: implications for the Phanerozoic crustal growth of Central Asia [J]. *Journal of Asian Earth Sciences*, 2002, 21: 87–110.
- [8] Xiao W J, Windley B F, Hao J, et al. Accretion leading to collision and the Permian Solonker suture, Inner Mongolia, China: Termination of the central Asian orogenic belt [J]. *Tectonics*, 2003, 22(6): 1069, doi: 10.1029/2002TC001484.
- [9] Xiao W J, Windley B F, Huang B C, et al. End–Permian to mid-Triassic termination of the accretionary processes of the southern Altaiids: implications for the geodynamic evolution, Phanerozoic continental growth, and metallogeny of Central Asia [J]. *International Journal of Earth Sciences*, 2009, 98: 1189–1217.
- [10] Wilhem C, Windley B F, Stampfli G M. The Altaiids of Central Asia: A tectonic and evolutionary innovative review [J]. *Earth Science Reviews*, 2012, 113: 303–341.
- [11] Kröner A, Kovach V, Belousova E, et al. The Altaiids of Central Asia: A tectonic and evolutionary innovative review [J]. *Gondwana Research*, 2014, 25: 103–125.
- [12] Li J Y. Permian geodynamic setting of Northeast China and adjacent regions: Closure of the Paleo–Asian Ocean and subduction of the Paleo–Pacific Plate [J]. *Journal of Asian Earth Sciences*, 2006, 26: 207–224.
- [13] 唐克东. 中朝陆台北侧褶皱带构造发展的几个问题[J]. 现代地质, 1989, 3(2): 195–204.
Tang Kedong. On tectonic development of the fold belts in the north margin of Sino–Korean platform [J]. *Geoscience*, 1989, 3 (2): 195–204 (in Chinese with English abstract).
- [14] 邵济安. 中朝板块北缘中段地壳演化[M]. 北京: 北京大学出版社, 1991.
Shao Ji'an. Crust Evolution in the Middle Part of the Northern Margin of Sino–Korean Plate [M]. Beijing: Peking University Publishing House, 1991 (in Chinese).
- [15] 王荃. 内蒙古中部中朝与西伯利亚古板块间缝合线的确定[J]. 地质学报, 1986, 1: 31–43.
Wang Quan. Recognition of the suture between the Sino–Korean and Siberian paleoplates in the middle part of Inner Mongolia [J]. *Acta Geologica Sinica*, 1986, 1: 31–43 (in Chinese with English abstract).
- abstract).
- [16] 王荃, 刘雪亚, 李锦轶. 中国内蒙古中部的古板块构造[J]. 中国地质科学院院报, 1991, 22: 1–15.
Wang Quan, Liu Xueya, Li Jinyi. Paleoplate tectonics in Nei Monggol of China [J]. *Bulletin of the Chinese Academy of Geological Sciences*, 1991, 22: 1–15 (in Chinese with English abstract).
- [17] 王玉净, 樊志勇. 内蒙古西拉木伦河北部蛇绿岩带中二叠纪放射虫的发现及其地质意义[J]. 古生物学报, 1997, 36(1): 58–68.
Wang Yujing, Fan Zhiyong. Discovery of Permian radiolarians in ophiolite belt on northern side of Xarmoron river, Nei Monggol and its geological significance [J]. *Acta Palaeontologica Sinica*, 1997, 36: 58–69 (in Chinese with English abstract).
- [18] 缪立春, 张海峰, 方伟明, 等. Geochronology and geochemistry of the Hegenshan ophiolitic complex: Implications for late– stage tectonic evolution of the Inner Mongolia–Daxinganling Orogenic Belt, China [J]. *Journal of Asian Earth Sciences*, 2008, 32: 348–370.
- [19] 詹平, 刘大勇, Kröner A, et al. Time scale of an early to mid-Paleozoic orogenic cycle of the long– lived Central Asian Orogenic Belt, Inner Mongolia of China: Implications for continental growth [J]. *Lithos*, 2008, 101(3/4): 233–259.
- [20] 詹平, 刘大勇, Kröner A, et al. Evolution of a Permian intraoceanic arc– trench system in the Solonker suture zone, Central Asian Orogenic Belt, China and Mongolia [J]. *Lithos*, 2010, 118: 169–190.
- [21] 黄本宏, 丁秋红. 中国北方安加拉植物群[J]. 地球学报, 1998, 19 (1): 97–104.
Huang Benhong, Ding QiuHong. The Angara flora from northern China [J]. *Acta Geoscientia Sinica*, 1998, 19(1): 97–104 (in Chinese with English abstract).
- [22] 尚启海. Occurrences of Permian radiolarians in central and eastern Nei Mongol (Inner Mongolia) and their geological significance to the Northern China Orogen [J]. *Chinese Science Bulletin*, 2004, 49 (24): 2613–2619.
- [23] 和政军, 刘淑文, 任纪舜, 等. 内蒙古林西地区晚二叠世—早三叠世沉积演化及构造背景[J]. 中国区域地质, 1997, 16(4): 403–409.
He Zhengjun, Liu Shuwen, Ren Jishun, et al. Late Permian–Early Triassic sedimentary evolution and tectonic setting of the Linxi region, Inner Mongolia [J]. *Regional Geology of China*, 1997, 16 (4): 403–409 (in Chinese with English abstract).
- [24] 李朋武, 高锐, 管烨, 等. 内蒙古中部索伦—林西缝合带封闭时代的古地磁分析[J]. 吉林大学学报(地球科学版), 2006, 36 (5): 744–758.
Li Pengwu, Gao Rui, Guan Ye, et al. Palaeomagnetic constraints on the final closure time of Solonker–Linxi Suture [J]. *Journal of Jilin University (Earth Science Edition)*, 2006, 36 (5): 744–758 (in Chinese with English abstract).
- [25] 王成文, 金巍, 张兴洲, 等. 东北及邻区晚古生代大地构造属性新认识[J]. 地层学杂志, 2008, 32(2): 119–136.
Wang Chengwen, Jin Wei, Zhang Xingzhou, et al. New understanding of the Late Paleozoic tectonics in northeastern

- China and adjacent areas [J]. *Journal of Stratigraphy*, 2008, 32(2): 119–136 (in Chinese with English abstract).
- [26] 曹从周, 杨芳林, 田昌裂, 等. 内蒙古贺根山地区蛇绿岩及中朝板块和西伯利亚板块之间的缝合带位置[C]//中国北方板块构造造论文集编委会编. 中国北方板块构造论文集(第一集). 北京: 地质出版社, 1986: 64–86.
- Cao Congzhou, Yang Fanglin, Tian Changlie, et al. The ophiolite in Hegenshan district, Nei Mongol and the position of suture line between Sino-Korean and Siberian plate [C]//Editorial Committee of Plate Tectonics Corpus in the North of China. *Plate Tectonics Corpus in the North of China*. Beijing: Geological Publishing House, 1986: 64–86 (in Chinese with English abstract).
- [27] 包志伟, 陈森煌, 张桢堂. 内蒙古贺根山地区蛇绿岩稀土元素和 Sm–Nd 同位素研究[J]. *地球化学*, 1994, 23(4): 339–349.
- Bao Zhiwei, Chen Senhuang, Zhang Zhentang. Study on REE and Sm–Nd isotopes of Hegenshan ophiolite, Inner Mongolia [J]. *Geochimica*, 1994, 23(4): 339–349 (in Chinese with English abstract).
- [28] 梁日暄. 内蒙古中段蛇绿岩特征及地质意义[J]. *中国区域地质*, 1994, (1): 37–45.
- Liang Rixuan. The features of ophiolites in the Central sector of Inner Mongolia and its geological significance [J]. *Regional Geology of China*, 1994, (1): 37–45 (in Chinese with English abstract).
- [29] Robinson P T, Zhou M F, Hu X F, et al. Geochemical constraints on the origin of the Hegenshan Ophiolite, Inner Mongolia, China [J]. *Journal of Asian Earth Sciences*, 1999, 17 (4): 423–442.
- [30] Xu B, Chen B. Framework and evolution of the middle Paleozoic orogenic belt between Siberian and North China Plates in northern Inner Mongolia [J]. *Science in China (Series D)*, 1997, 40 (5): 463–469.
- [31] 徐备, 赵盼, 鲍庆中, 等. 兴蒙造山带前中生代构造单元划分初探[J]. *岩石学报*, 2014, 30(7): 1841–1857.
- Xu Bei, Zhao Pan, Bao Qingzhong, et al. Preliminary study on the pre-Mesozoic tectonic unit division of the Xing-Meng Orogenic Belt (XMOB). *Acta Petrologica Sinica*, 2014, 30(7): 1841–1857 (in Chinese with English abstract).
- [32] Xu B, Zhao P, Wang Y Y, et al. The pre-Devonian tectonic framework of Xing'an-Mongolia orogenic belt (XMOB) in north China [J]. *Journal of Asian Earth Sciences*, 2015, 97: 183–196.
- [33] Liu J F, Li J Y, Chi X G, et al. A late-Carboniferous to early-early-Permian subduction-accretion complex in Daqing pasture, southeastern Inner Mongolia: Evidence of northward subduction beneath the Siberian paleoplate southern margin [J]. *Lithos*, 2013, 177: 285–296.
- [34] Song S G, Wang M M, Xu X, et al. Ophiolites in the Xing'an-Inner Mongolia accretionary belt of the CAOB: Implications for two cycles of seafloor spreading and accretionary orogenic events [J]. *Tectonics*, 2015, 34(10): 2221–2248.
- [35] Zhang Z C, Li K, Li J F, et al. Geochronology and geochemistry of the Eastern Erenhot ophiolitic complex: Implications for the tectonic evolution of the Inner Mongolia-Daxinganling Orogenic Belt [J]. *Journal of Asian Earth Sciences*, 2015, 97: 279–293.
- [36] 黄波, 付冬, 李树才, 等. 内蒙古贺根山蛇绿岩形成时代及构造启示[J]. *岩石学报*, 2016, 32(1): 158–176.
- Huang Bo, Fu Dong, Li Shuai, et al. The age and tectonic implications of the Hegenshan ophiolite in Inner Mongolia [J]. *Acta Petrologica Sinica*, 2016, 32(1): 158–176 (in Chinese with English abstract).
- [37] 李锦铁, 高立明, 孙桂华, 等. 内蒙古东部双井子中三叠世同碰撞壳源花岗岩的确定及其对西伯利亚与中朝古板块碰撞时限的约束[J]. *岩石学报*, 2007, 23 (3): 565–582.
- Li Jinyi, Gao Liming, Sun Guihua, et al. Shuangjingzi middle Triassic syn-collisional crust-derived granite in the east Inner Mongolia and its constraint on the timing of collision between Siberian and Sino-Korean paleo-plates [J]. *Acta Petrologica Sinica*, 2007, 23(3): 565–582 (in Chinese with English abstract).
- [38] Zhang S H, Zhao Y, Song B, et al. Carboniferous granitic plutons from the northern margin of the North China block: implications for a late Palaeozoic active continental margin [J]. *Journal of the Geological Society*, 2007, 164: 451–463.
- [39] Zhang S H, Zhao Y, Song B, et al. Contrasting Late Carboniferous and Late Permian–Middle Triassic intrusive suites from the northern margin of the North China craton: Geochronology, petrogenesis, and tectonic implications [J]. *Bulletin of the Geological Society of America*, 2009, 121(1/2): 181–200.
- [40] 刘建峰, 迟效国, 张兴洲, 等. 内蒙古西乌旗南部石炭纪石英闪长岩地球化学特征及其构造意义[J]. *地质学报*, 2009, 83(3): 365–376.
- Liu Jianfeng, Chi Xiaoguo, Zhang Xingzhou, et al. Geochemical characteristic of Carboniferous quartz-diorite in the Southern Xiuqi Area, Inner Mongolia and its tectonic significance [J]. *Acta Geologica Sinica*, 2009, 83(3): 365–376 (in Chinese with English abstract).
- [41] 李文国, 李庆富, 姜万德, 等. 内蒙古自治区岩石地层[M]. 武汉: 中国地质大学出版社, 1996.
- Li Wenguo, Li Qingfu, Jiang Wande, et al. *The Strata of Inner Mongolian Autonomous Region* [M]. Wuhan: China University of Geosciences Press, 1996 (in Chinese).
- [42] Zhang Y S, Tian S G, Li Z S, et al. Discovery of marine fossils in the upper part of the Permian Linxi Formation in Lopingian, Xingmeng area, China [J]. *Chinese Science Bulletin*, 2014, 59(1): 62–74.
- [43] 宋彪, 张玉海, 万渝生, 等. 锆石 SHRIMP 样品靶制作、年龄测定及有关现象讨论[J]. *地质论评*, 2002, 48(增刊): 26–30.
- Song Biao, Zhang Yuhai, Wan Yusheng, et al. Mount making and procedure of the SHRIMP dating [J]. *Geological Review*, 2002, 48 (Supp.), 26–30 (in Chinese with English abstract).
- [44] Liu Y S, Hu Z C, Zong K Q, et al. Reappraisal and refinement of zircon U-Pb isotope and trace element analyses by LA-ICP-MS [J]. *Chinese Science Bulletin*, 2010, 55(15): 1535–1546.
- [45] Liu Y S, Hu Z C, Gao S, et al. In situ analysis of major and trace elements of anhydrous minerals by LA-ICP-MS without applying an internal standard [J]. *Chemical Geology*, 2008, 257 (1–2): 34–43.

- [46] Ludwig K R. Isoplot/Ex rev.2.49: A Geochronological Toolkit for Microsoft Excel [M]. Berkeley Geochronology Center Special Publication No. 1a, 2001, 1–58.
- [47] Wu Y B, Zheng Y F. Genesis of zircon and its constraints on interpretation of U–Pb age [J]. Chinese Science Bulletin, 2004, 49(15): 1554–1569.
- [48] 何国琦, 邵济安. 内蒙东南部(昭盟)西拉木伦河一带早古生代蛇绿岩建造的确认及其大地构造意义[C]//唐克东(主编). 中国北方板块构造文集(1). 北京: 地质出版社, 1983: 243–249.
He Guoqi, Shao Ji’ an. Determination of Early Paleozoic ophiolites in southeastern Nei Mongol and their geotectonic significance [C]//Tang Kedong (eds.). Contributions for the Project of Plate Tectonics in Northern China (No.1). Beijing: Geological Publishing House, 1983: 243–249 (in Chinese with English abstract)
- [49] 陈森煌, 刘道荣, 包志伟, 等. 华北地台北缘几个超基性岩带的侵位年代及其演化[J]. 地球化学, 1991, (2): 128–133.
Chen Senhuang, Liu Daorong, Bao Zhiwei, et al. Emplacement ages and evolution of several ultrabasic rock belts on the northern margin of the North China platform [J]. Geochimica, 1991, (2): 128–133 (in Chinese with English abstract).
- [50] 孔庆玉, 龚与觐. 苏皖地区下二叠统放射虫硅质岩形成环境探讨[J]. 石油与天然气地质, 1987, 8(1): 86–89.
Kong Qingyu, Gong Yujin. The formation environment of radiolarian siliciliths in the Lower Permian in Jiangsu–Anhui region [J]. Oil and Gas Geology, 1987, 8(1): 86–89 (in Chinese with English abstract).
- [51] 王博, 舒良树. 对赣东北晚古生代放射虫的初步认识[J]. 地质论评, 2001, 47(4): 337–344.
Wang Bo, Shu Liangshu. Notes on Late Paleozoic radiolarians of northeastern Jiangxi Province[J]. Geological Review, 2001, 47(4): 337–344 (in Chinese with English abstract).
- [52] 方俊钦, 赵盼, 徐备, 等. 内蒙古西乌珠穆沁旗哲斯组宏体化石新发现和沉积相分析[J]. 岩石学报, 2014, 30(7): 1889–1898.
Fang Junqin, Zhao Pan, Xu Bei, et al. Sedimentary facies analyses and discovery of gastropods from Zhesi formation in the south of West Ujimqin, Inner Mongolia and their significances[J]. Acta Petrologica Sinica, 2014, 30(7): 1889–1898 (in Chinese with English abstract).
- [53] 舒良树, 王玉净. 新疆卡拉麦里蛇绿岩带中硅质岩的放射虫化石[J]. 地质论评, 2003, 49(4): 408–412.
Shu Liangshu, Wang Yujing. Late Devonian–Early Carboniferous Radiolarian Fossils from siliceous rocks of the Kelameili Ophiolite, Xinjiang [J]. Geological Review, 2003, 49(4): 408–412 (in Chinese with English abstract).
- [54] 舒良树, 王博, 朱文斌. 南天山蛇绿混杂岩中放射虫化石的时代及其构造意义[J]. 地质学报, 2007, 81(9): 1161–1168.
Shu Liangshu, Wang Bo, Zhu Wenbin. Age of radiolarian fossils from the Heiyingshan Ophiolitic Mélange, Southern Tianshan Belt, NW China, and its tectonic significance [J]. Acta Geologica Sinica, 2007, 81(9): 1161–1168 (in Chinese with English abstract).
- [55] Zhang N, Xia W C, Dong Y X, et al. Conodonts and radiolarians from pelagic cherts of the Frasnian–Famennian boundary interval at Bancheng, Guangxi, China: Global recognition of the upper Kellwasser event[J]. Marine Micropaleontology, 2008, 67(1/2): 180–190.
- [56] Liu J F, Li J Y, Chi X G, et al. The tectonic setting of early Permian bimodal volcanism in central Inner Mongolia: continental rift, post–collisional extension, or active continental margin? [J]. International Geology Review, 2016, 58(6): 737–755.
- [57] Liu J F, Chi X G, Zhao Z, et al. Geochemical Characteristics and Geological Significance of Early Permian Baya’ertuhushuo Gabbro in South Great Xing’ an Range [J]. Acta Geologica Sinica, 2011, 85(1): 116–129.
- [58] 刘建峰, 李锦轶, 迟效国, 等. 华北克拉通北缘与弧–陆碰撞相关的早泥盆世长英质火山岩——锆石U–Pb定年及地球化学证据[J]. 地质通报, 2013, 32(2–3): 267–278.
Liu Jianfeng, Li Jinyi, Chi Xiaoguo, et al. Early Devonian felsic volcanic rocks related to the arc–continent collision on the northern margin of North China craton—evidences of zircon U–Pb dating and geochemical characteristics [J]. Geological Bulletin of China, 2013, 32(2–3): 267–278 (in Chinese with English abstract).
- [59] Zhang Wei, Jian Ping, Kröner Alfred, et al. Magmatic and metamorphic development of an early to mid–Paleozoic continental margin arc in the southernmost Central Asian Orogenic Belt, Inner Mongolia, China [J]. Journal of Asian Earth Sciences, 2013, 72(10): 63–74.
- [60] Li W B, Zhong R C, Xu C, et al. U–Pb and Re–Os geochronology of the Bainaimiao Cu–Mo–Au deposit, on the northern margin of the North China Craton, Central Asia Orogenic Belt: Implications for ore genesis and geodynamic setting [J]. Ore Geology Reviews, 2012, 48: 139–150.
- [61] 张海华, 郑月娟, 陈树旺, 等. 大兴安岭南部幸福之路组的时代及二叠–三叠系界线研究——来自凝灰岩LA–ICP–MS锆石U–Pb年龄的证据[J]. 中国地质, 2015, (6): 1754–1764.
Zhang Haihua, Zheng Yuejuan, Chen Shu旺, et al. Age of Xingfuzhilu Formation and contact relationship between Permian and Triassic strata in southern Da Hinggan Mountains: Constraints from the tuff zircon U–Pb ages [J]. Geology in China, 2015, (6): 1754–1764 (in Chinese with English abstract).
- [62] 刘建峰, 迟效国, 赵芝, 等. 内蒙古巴林右旗建设屯埃达克岩锆石U–Pb年龄及成因讨论[J]. 岩石学报, 2013, 29(3): 827–839.
Liu Jianfeng, Chi Xiaoguo, Zhao Zhi, et al. Zircon U–Pb age and petrogenetic discussion on Jianshetun adakite in Balinyouqi, Inner Mongolia [J]. Acta Petrologica Sinica, 2013, 29(3): 827–839 (in Chinese with English abstract).
- [63] 刘建峰, 李锦轶, 迟效国, 等. 内蒙古东南部早三叠世花岗岩带岩石地球化学特征及其构造环境[J]. 地质学报, 2014, 88(9): 1677–1690.
Liu Jianfeng, Li Jinyi, Chi Xiaoguo, et al. Petrological and geochemical characteristics of the Early Triassic granite belt from southeast Inner Mongolia and its tectonic setting [J]. Acta Geologica Sinica, 2014, 88(9): 1677–1690 (in Chinese with English abstract).